GROWTH OF PLASTIC STRAIN AT THE VERTEX OF A CRACK IN A CRYSTAL IN ANTIPLANAR SHEARING

D. N. Karpinskii and S. V. Sannikov

UDC 539.4.015

A stress concentration is produced by an external load at the vertex of a crack in a crystal, which relaxes by plastic strain [1]. The region involved in the plastic strain is called the plastic zone, whose shape and strain distribution are determined by the stress distribution and the properties of the crystal.

One usually distinguishes two major parts of the plastic zone: the plastic zone proper, which occupies much of the plastic region at the vertex, and a minor zone lying directly ahead of the vertex, which in the foreign literature [2] is called the failure zone, while in [3] we find the proposed name instability zone. The strain in this zone is usually substantially larger than that in the rest of the plastic zone. The main part in the instability zone is played by the rotational plastic deformation mode, which is accompanied by the initiation and growth of microcracks [4-6].

Sometimes there is no plastic strain at the very vertex of the crack (a zone free from dislocations) [7, 8].

Calculations have been performed [9-12] on the shape of the plastic zone and the strain distribution in it on the basis of a mechanical equation of state relating the local plastic strain ε to the stress σ at that point.

This serves to explain some features of the plastic zone, but it does not incorporate the time course of the plastic strain or the nonlocal character of it [the stress in a given volume element $dV(\mathbf{r})$ is dependent not only on the strain at point $\mathbf{r}$ but also on the strain distribution in adjacent areas]. In [13], a study was made of the time evolution of the plastic zone at constant stress, but no allowance was made for the nonlocal character of the stress in the plastic zone or for the strain distribution there.

We have used computer simulation to establish the time-dependent trends in the plastic zone giving rise to the nonlocal strain.

Consider an unbounded bcc crystal containing a rectilinear crack of length 2L, which lies in the (010) cleave plane y = 0 with its vertex at x = 0 (Fig. 1). The shearing stress $\sigma_{yz} = \sigma_a'$ is applied at infinity, which is sufficient to produce a plastic zone but insufficient for the crack to grow.

We assume that the crystal contains uniformly distributed sources of Frank—Reed dislocations, which emit dislocation loops under the shear stress in the {110} easy-slip planes. We

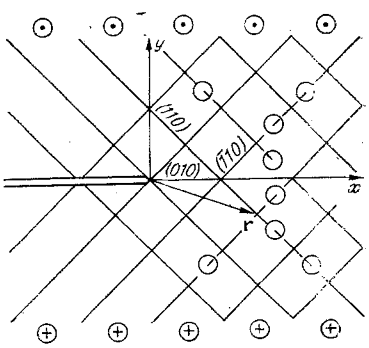

Fig. 1

Rostov-on-Don. Translated from Zhurnal Prikladnoi Mekhaniki i Tekhnicheskoi Fiziki, No. 2, pp. 160-164, March-April, 1986. Original article submitted February 6, 1985.

assume that these loops are rectangular and elongated parallel to the crack vertex. To simplify the calculations, we assume that the segments of the loops parallel to the crack vertex have only a screw component, with Burgers vector 1/2[001], while we neglect the segments perpendicular to this. This simplification allows us to use a planar treatment.

The plastic-strain rate in the volume dV(r) is determined by the dislocation motion in the {110} slip planes, which involves thermally activated barrier transit [14, 15]:

$$\frac{d\varepsilon}{dt} = \dot{\varepsilon}_0 \exp\left\{-\frac{U_0(1-(\sigma_e/\tau_0))^{1/2}}{kT}\right\}, \tag{1}$$

where $\dot{\varepsilon}_0 = 10^{11}$ sec^{-1}, τ_0 is a constant, U_0 is activation energy, k is Boltzmann's constant, T is temperature, and σ_e the effective tangential stress in the slip plane:

$$\sigma_e = \sigma_c(\mathbf{r}) + \sigma_0 + \sigma_f(\mathbf{r}) + \sigma_l(\mathbf{r}). \tag{2}$$

All the terms in (2) relate to these slip planes. Here σ_c is the stress external to the given volume element calculated from Westergard's formulas [16] (planar deformation), which do not incorporate plastic relaxation and which lead to excessively large stresses in a region of radius R* around the crack vertex. We therefore write σ_c in the form

$$\sigma_c(\mathbf{r}) = \sigma_a' \sqrt{L}\,(R_0 + r)^{-1/2} f(\theta), \quad r < R^*; \quad R_0 = 0, \quad r \geqslant R^*, \tag{3}$$

where $f(\theta)$ is the angular part of the Westergard formula; R_0, radius of curvature at the vertex; $\sigma_s = \sigma_0 + \sigma_f$, short-range stresses that retard dislocations due to lattice friction σ_0 and intersection with forest dislocations of density ρ; $\sigma_f = \alpha G b\sqrt{\rho}$; α, parameter of the order of one; G, shear modulus. Subsequently, σ_f is replaced by the empirical relation $\sigma_f = \sigma_1 \varepsilon^n$, where σ_1 and n are constants and σ_ℓ is the long-range stress due to excess dislocations of one sign and density $\Delta\rho$ lying at the points **r'**:

$$\sigma_l(\mathbf{r}) = \int_S d\mathbf{r}' F(\mathbf{r}, \mathbf{r}')\, \Delta\rho(\mathbf{r}'). \tag{4}$$

Here F is the Green's function for an infinite elastic medium having a semiinfinite slot containing a source of stress at point r' [17]:

$$F(\mathbf{r}, \mathbf{r}') = \frac{Gb}{4\pi}\left[\sqrt{\frac{z'}{z}}\,\frac{1}{z - z'} + \sqrt{\frac{\bar{z}'}{z}}\,\frac{1}{z - \bar{z}'}\right], \quad z = x + iy. \tag{5}$$

The integration is carried over the entire area S of the plastic zone. The density $\Delta\rho$ is defined by the inhomogeneity in the plastic strain [18]

$$\Delta\rho = -\mathbf{b}^{-1}(\nabla \times \varepsilon), \tag{6}$$

where **b** is the dislocation Burgers vector.

Equations (1)-(6) form a system that can be solved with given values for the constants and the following initial conditions: at time t = 0, the strain $\varepsilon = 0$, and a tensile stress $\sigma_a' < \sigma$ is applied. The values of σ_a' is taken in accordance with

$$\sigma_a'(t + \Delta t) = \dot{\sigma}_a \Delta t_i + \sigma_a'(t), \tag{7}$$

where $\dot{\sigma}_a$ is the given loading rate and Δt_i is the time step; $\sigma_a(0) = 0.1\sigma_m$, with σ_m the applied shear stress giving the maximum strain rate $\dot{\varepsilon}_{max} = 0.1$ sec^{-1}. When the maximum strain rate is attained during loading, the loading rate $\dot{\sigma}_a$ is reduced by an order of magnitude. The stress σ_a' increases to the set σ_a, after which the external load is fixed until equilibrium in the plastic strain is attained. Here Δt_i is chosen automatically from the condition for σ_e to increase by its set amount in a time from t to t + dt.

The cross section of the crystal was split up into square cells of side ℓ to integrate (1)-(7); within each cell we took the calculated quantities as constant and equal to their values at a node in the computational net. By virtue of the symmetry, we consider only the upper half of the crystal (relative to the crack).

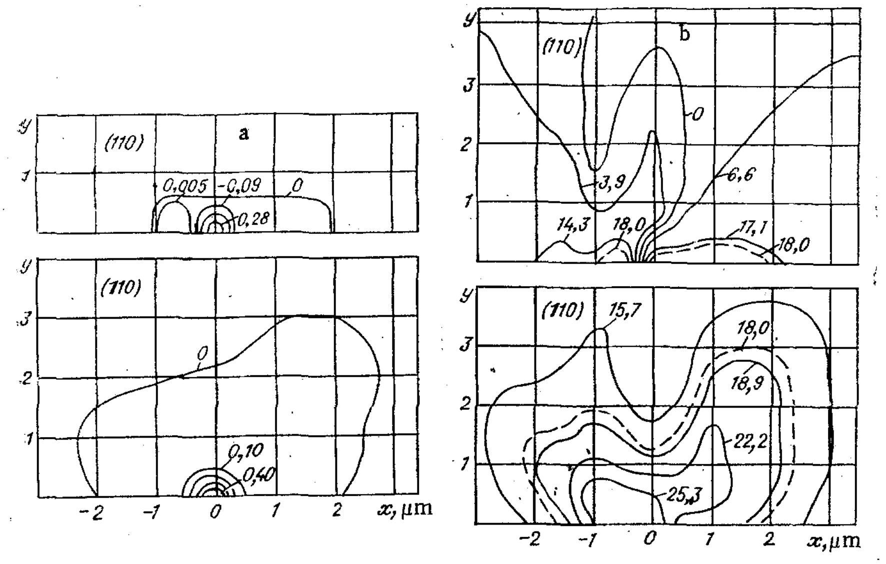

Fig. 2

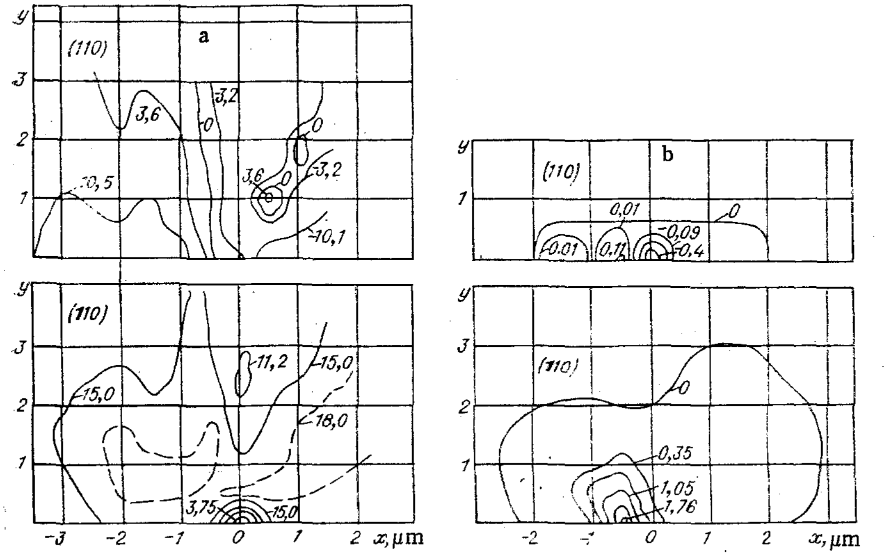

Fig. 3

To derive $\varepsilon(t_i)$, we substituted $\sigma(t_i - 1)$ on the right; the initial step $\Delta t = t_1$ was taken such that the stress relaxation in this time can be neglected on the basis that

$$\varepsilon_1(t_0, \mathbf{r}) = t_1 \dot{\varepsilon}_0 \exp\left\{-\frac{U_0\left(1-\left(\sigma_e^{(0)}/\tau_0\right)\right)^{1/2}}{kT}\right\} \operatorname{sign} \sigma_e^{(0)},$$

where $\sigma_e^{(0)} = \sigma_c^{(0)}(\mathbf{r}) - \sigma_0 \operatorname{sign} \sigma_c$ for $|\sigma_c| > \sigma_0$ and $\sigma_e^{(0)} = 0$ for $|\sigma_c| \leq \sigma_0$. The subsequent calculation was on an explicit scheme with automatic step selection:

$$\varepsilon_i(t_i, \mathbf{r}) = (t_i - t_{i-1}) \dot{\varepsilon}_0 \exp\left\{-\frac{U_0\left(1-\left(\sigma_e^{(i-1)}/\tau_0\right)\right)^{1/2}}{kT}\right\} \operatorname{sign} \sigma_e^{(i-1)} + \varepsilon_{i-1},$$

where $\sigma_e^{(i-1)} = \sigma_c^{(i-1)}(\mathbf{r}) + \sigma_l^{(i-1)}(\mathbf{r}) - (\sigma_0 + \sigma_f) \operatorname{sign}\left(\sigma_c^{(i-1)} + \sigma_l^{(i-1)}\right)$ for $|\sigma_c^{(i-1)} + \sigma_l^{(i-1)}| > \sigma_0 + \sigma_f$ and $\sigma_e^{(i-1)} = 0$ for $|\sigma_c^{(i-1)} + \sigma_l^{(i-1)}| < \sigma_0 + \sigma_f$. In the calculations, we neglected increments in the plastic strain less than 10^{-6}.

We selected the following parameters for α-Fe for the numerical calculations: $U_0 = 0.9$ eV, $\tau_0 = 330$ MPa [15], $\dot{\sigma} = 2$ kgf/sec·mm², shear modulus in the {110} plane G = 60 GPa [19], Poisson's ratio $\nu = 0.3$, and yield point $\sigma_0 = 18$ MPa. Crack length 1 mm, radius of curvature at vertex $R_0 = 0.1$ μm, maximum applied stress $\sigma_a = 1.4$ MPa, temperature T = 300 K, cell size $\ell = 0.5$ μm, n = 1, and $\sigma_1 = 10^3$ MPa.

This gave $\sigma = \sigma_c - \sigma_\ell - \sigma_f \operatorname{sign} \varepsilon$, together with the strains at the vertex at various instants. Figures 2 and 3 show that σ_ℓ arising from the accumulation of extensive dislocation charges plays a substantial part in the thermally activated plastic strain at the vertex with this model. In the initial period, where σ_ℓ is small (the dislocation charges are weak), the plastic zone gradually expands, while the shape changes in a self-similar fashion. As the plastic zone expands further, the second stage gradually sets in, where σ_ℓ makes the main contribution to (2). In this stage, the strain is substantially redistributed in the plastic zone. Figures 2a and 3a show lines of equal plastic strain at the vertex for t = 0.17 and 11.8 sec. The numbers on the isolines indicate the corresponding strains in percent. Figures 2b and 3b show the lines of equal stress for the same instants. The numbers on the isolines indicate σ in megapascals. At t = 0.17 sec, the plastic strain occurs in the regions delineated by the dashed lines, where the stress is above the yield point. At t = 18 sec, the stress has become less than the yield point and the plastic strain has attained equilibrium.

Figure 2 shows that the peak plastic strain at the initial instant lies at the crack vertex, while the effective stress defining the shape of the plastic zone and the strain distribution in it is in the main described by σ_c. In the closing stage of plastic-zone formation (Fig. 3), the peak strain (1.7%) is displaced from the vertex by about 1-2 μm, while the region directly adjoining the vertex is unstressed. These results indicate that the model partially describes the dislocation-free region occurring within the plastic zone [7, 8]. One expects that better agreement between theory and experiment would be possible if one incorporates the penetration of the dislocations into the crack and the emission of dislocations by the vertex.

In [20], the parameters of the dislocation-free zone and plastic zone were calculated from a model that did not incorporate the image forces. This calculation shows that the dislocation penetration mechanism considered in [20] to explain the dislocation-free region is substantially supplemented if one incorporates the image forces.

Thus, if one allows for the long-range stress due to the accumulation of dislocations of one sign, one has a substantially modified conception of the plastic-zone structure as a passive element controlled only by the elastic stress of the crack σ_c. On the other hand, in the final stage of plastic-zone formation, the stress σ_ℓ largely controls the evolution of the plastic strain.

LITERATURE CITED

1. P. I. Vitvitskii, V. V. Panasyuk, and S. Ya. Yarema, "Plastic strain near a crack and failure criteria," Probl. Prochn., No. 2 (1973).
2. I. C. Howard and A. A. Willoughby, "Mechanics and mechanisms of ductile fracture," in: Development in Fracture Mechanics, Vol. 2, London—New Jersey (1981).
3. V. I. Vladimirov, D. N. Karpinskii, et al., "Computer simulation of strain kinetics in the plastic zone at a crack vertex," Probl. Prochn., No. 12 (1983).
4. Yu. I. Poluéktov and V. V. Rybin, "Plastic crack growth," Fiz. Met. Metalloved., 34, No. 6 (1972).
5. V. I. Vladimirov and N. D. Priemskii, "Microscopic discontinuities in the plastic zone ahead of a crack vertex," Fiz. Tverd. Tela, No. 12 (1982).
6. V. V. Rybin, A. A. Zisman, and I. M. Zhukovskii, "Microcrack formation under conditions of developed plastic strain," Probl. Prochn., No. 12 (1982).
7. S. Kobayashi and S. M. Ohr, "In situ fracture experiments in bcc metals," Philos. Mag., A42, 763 (1980).
8. S. J. Chang and S. M. Ohr, "Dislocation-free zone models of fracture," J. Appl. Phys., 52, 7174 (1971); "Dislocation-free zone models of fracture: comparison with experiments," J. Appl. Phys., 53, 5645 (1982).
9. J. R. Rice and G. F. Rosengren, "Plane strain deformation near a crack tip in a power-law hardening material," J. Mech. Phys. Sol., 16, 1 (1968).
10. J. W. Hutchinson, "Singular behavior at the end of a tensile crack in hardening material," J. Mech. Phys. Sol., 16, 13 (1968).
11. V. A. Kudryavtsev and V. Z. Parton, "The local plastic zone near the end of a slot," Izv. Akad. Nauk SSSR, Mekh. Tverd. Tela, No. 1 (1970); "The local plastic zone near the end of a slot (planar deformation)," Izv. Akad. Nauk SSSR, Mekh. Tverd. Tela, No. 5 (1970).
12. V. Vitek, "Yielding on inclined planes at the tip of a crack loaded in uniform tension," J. Mech. Phys. Sol., 24, 263 (1976).

13. J. L. Bassoni and F. A. McClintok, "Creep relaxation of stress around a crack tip," Int. J. Sol. Struct., 17, 479 (1981).
14. R. Berner and H. Kronmüller, Plastic Strain in Single Crystals [Russian translation], Mir, Moscow (1969).
15. W. A. Spitzig, "Analysis of the plastic deformation in iron single crystals," Acta Met., 18, 1275 (1970).
16. H. M. Westergard, "Bearing pressure and crack," J. Appl. Mech., 6, 220 (1939).
17. E. W. Hart, "A theory for stable crack extension rates in ductile materials," Int. J. Sol. Struct., 16, 807 (1980).
18. E. Kröner, Kontiniumtheorie der Versetzungen und Eigenspannungen, Springer-Verlag, Berlin (1958).
19. B. L. Auerbach, "Some physical aspects of failure," in: Failure [Russian translation], Vol. 1, Mir, Moscow (1973).
20. C. W. Lung and L. Y. Xiong, "The dislocation function in the plastic zone at a crack tip," Phys. Stat. Sol. (a), 77, 81 (1983).